Fabrication of layer-by-layer assembled FO hollow fiber membranes and their performances using low concentration draw solutions

Liu, Chang; Fang, Wangxi; Chou, Shuren; Shi, Lei; Fane, Anthony Gordon; Wang, Rong

2012

Liu, C., Fang, W., Chou, S., Shi, L., Fane, A. G., & Wang, R. (2012). Fabrication of layer-by-layer assembled FO hollow fiber membranes and their performances using low concentration draw solutions. Desalination, 308, 147-153.

https://hdl.handle.net/10356/96651

https://doi.org/10.1016/j.desal.2012.07.027

Fabrication of layer-by-layer assembled FO hollow fiber membranes and their performances using low concentration draw solutions

Chang Liu, Wangxi Fang, Shuren Chou, Lei Shi, Anthony G. Fane, Rong Wang*

School of Civil and Environmental Engineering, Nanyang Technological University, Singapore 639798

Singapore Membrane Technology Centre, Nanyang Technological University, Singapore 639798

**Corresponding author at: School of Civil and Environmental Engineering, Nanyang Technological University, 639798 Singapore*

Email: rwang@ntu.edu.sg

Abstract

Great efforts from the membrane community have been devoted in developing suitable membranes for forward osmosis (FO) applications in recent years. In the current study, the layer-by-layer (LBL) polyelectrolyte assembly technique has been successfully applied onto a micorporous polyethersulfone(PES) hollow fiber substrate to make novel LBL hollow fiber membranes suitable for FO process for the first time. The FO performance of the LBL hollow fibers with different numbers of deposited layers has been evaluated using deionized (DI) water as the feed and $MgCl_2$ solution of various concentrations as the draw solution in both orientations. With 6 layers deposited and in the active layer facing draw solution (AL-facing-DS) orientation, the membrane showed high water fluxes of 14.6, 25.9 and 40.5 L/m^2 h with corresponding salt to water flux, J_s/J_v , ratio of 0.034, 0.066 and 0.201 g/L using 0.05, 0.1 and 0.5 M draw solution, respectively. These promising results demonstrate the potential application of the LBL hollow fibers in FO process using low concentration draw solutions, which can substantially reduce the draw solution replenishment, and the energy consumption for draw solution regeneration and separation.

Keywords: forward osmosis; layer-by-layer polyelectrolyte deposition; FO hollow fiber membrane; low concentration draw solution.

1. Introduction

Unlike conventional pressure-driven membrane separation processes such as reverse osmosis (RO) and nanofiltration (NF), the forward osmosis (FO) process utilizes osmotic pressure differences, generated by a high concentration solution (referred to as draw solution) and a low concentration feed stream, as the driving force for the net water transportation across a semi-permeable membrane. Over the last decade, the FO process has shown great potential for its high energy efficiency in various applications including desalination [1, 2], brine concentration [3, 4], waste water treatment [5, 6], and food processing [7, 8]. However, the lack of an adequate membrane is one of the biggest hindrances that impedes industrial applications of FO. The early studies [9-11] show that commercial RO membranes produce very low water flux in FO operation despite their excellent salt rejection. This lower-than-expected performance is due to the severe internal concentration polarization (ICP) caused by the thick support layer which greatly reduces the effective osmotic pressure difference across the membrane. Meanwhile, the only available commercial FO membrane made from cellulose triacetate (CTA) by Hydration Technology Inc (HTI) presents relatively modest performance in various applications because of the high reverse salt flux [11-13].

Extensive efforts have been made by researchers from the membrane community in fabrication of novel membranes for the FO process, and the preparations of RO-like and NF-like membranes with improved structure parameters are the most commonly adopted approaches. In the former approach, thin film composite (TFC) membranes which are able to effectively reject monovalent ions such as Na^+ and Cl^- are made using the interfacial polymerization technique [14-17]. In contrast, the NF-like FO membranes have high rejection of multivalent ions like Mg^{2+} and SO_4^{2-} but relatively low to modest rejection to the monovalent ions. Several types of NF-like FO membranes have been reported such as the integral asymmetric cellulose acetate (CA) membrane by phase inversion [18], the dual layer polybenzimidazole (PBI) hollow fibers via co-extrusion [19] and the poly (amide-imide) (PAI) membrane crosslinked with polyethyleneime (PEI) [20-22]. A novel dual-skin FO membrane with a combination of RO-like and NF-like skins has also been developed by our group [16].

In addition to the above mentioned methods, polyelectrolyte layer-by-layer (LBL) assembly is an alternative technique to form NF-like thin film composite membranes. The LBL type of NF membrane has been extensively studied and applied for many applications because of its highly controllable performance and simple procedures for membrane preparation [23-26]. However, most examples are in the flat sheet configuration, including the recently reported membranes made by depositing poly(allylamine hydrochloride) (PAH) and poly(styrenesulfonic acid) (PSS) multi-layers on a hydrolyzed polyacrylonitrile (PAN) flat sheet substrate for FO application [27]. According to the literature [28, 29], hollow fiber membranes possess significant advantages over flat sheet membranes in the FO process due to their high packing density, favorable flow pattern and self-supported structure.

Therefore, it is worthwhile to explore the possibility of applying the LBL deposition technique on a polymeric hollow fiber substrate to make NF-like thin film composite membranes and evaluate their performance in the FO process. To the best of our knowledge, such an effort has not been reported previously. In the current work, LBL hollow fibers with different numbers of deposited layers have been fabricated and their FO performance has been tested using deionized (DI) water as the feed and $MgCl_2$ solutions of various concentrations as the draw solution. Both active layer facing the draw solution (AL-facing-DS) and active layer facing the feed water (AL-facing-FW) orientations have been tested to explore the potential of the newly developed LBL hollow fibers for FO applications.

2. Materials and experiments

2.1. Materials

The polyethersulfone (PES) hollow fiber substrates were produced in-house (properties are presented in Section 3.1). Poly(allylamine hydrochloride) (PAH, PolyScience, Mw = 120-200kDa) and poly(styrenesulfonic acid) sodium salt (PSS, Alfa Aesar, Mw = 500kDa) were used to make polyelectrolyte solutions with sodium chloride (NaCl, Merck) as the supporting electrolyte. The pH of polyelectrolyte solutions was adjusted with diluted hydrochloric acid (HCl) or sodium hydroxide (NaOH) solution. NaCl, sodium sulfate (Na_2SO_4), magnesium sulfate ($MgSO_4$) and magnesium chloride

($MgCl_2$) (Merck) were used for NF and FO performance tests. DI water was produced by a Mili-Q system (Milipore,USA).

2.2. Layer-by-layer (LBL) deposition

The deposition conditions, which include polyelectrolyte type, concentration, pH value and supporting electrolyte concentration, etc., were chosen based on the best NF performance attained in our previous work. The dried hollow fibers were sealed into plastic membrane modules and then immersed into the polyanion PSS (0.02 M with 0.5 M NaCl at a pH around 9) and polycation PAH (0.02 M with 2.5 M NaCl at a pH around 4) solutions alternately to achieve the desired number of layers. The immersing times for the PSS and PAH solutions were 2 and 5 min, respectively, with 3 min DI water rinse in between. The schematic drawing of the deposition process is shown in Fig. 1. Membrane modules were then stored in DI water for NF and FO performance evaluation. Throughout the paper, one pair of (PSS/PAH) deposition is considered as 1 layer of polyelectrolytes and thus n-layer LBL membrane refers to the membrane with n pairs of (PSS/PAH) deposition. A n.5-layer LBL membrane signifies a membrane terminated with an additional PSS half-layer on top of the n-layer of polyelectrolytes.

2.3. Membrane characterization and performance evaluation

2.3.1. Characterization of membrane substrates and LBL membranes

A series of standard protocols for the membrane substrate characterization can be found elsewhere [29]. The cross-section structure of the substrate was examined by a Zeiss EVO 50 Scanning Electron Microscope (SEM). The porosity was determined by the gravimetric method, measuring the weight difference between the dry and 2-proponal wetted fibers. The pure water permeability (PWP, using DI water) and molecular weight cut-off tests (MWCO) using a mixed dextran solution were carried out on a bench scale cross-flow filtration unit at 1 bar. The MWCO was then determined by the gel permeation chromatography (GPC, Polymer Laboratories, GPC 50 plus system) [30]. The dried hollow fiber surface before and after LBL deposition was analyzed by Fourier transform infra red spectrometer (FTIR, Shimadzu IR Prestige-21) using attenuated total reflection (ATR) method.

2.3.2. Filtration measurement and FO performance tests

The salt water permeability (SWP) and salt rejection of the LBL hollow fiber membranes were determined by the same cross-flow filtration unit under 1 bar. Relatively high cross-flow velocity (Reynolds number of around 1500) was maintained for the salt solution flow to minimize the concentration polarization effect. The salt rejection tests were conducted using 500 ppm NaCl, Na_2SO_4, $MgSO_4$, $MgCl_2$ solutions, respectively, based on the conductivity measurements (Ultrameter II, Myron L Company, Carlsbad, CA) of the permeate and feed water.

Two FO orientations, the AL-facing-DS and AL-facing-FW, were tested using a lab-scale FO unit which is similar to the unit reported previously [31]. The Reynolds numbers of the fluids flowing in the lumen and shell side of the modules were kept at around 2000 to minimize external concentration polarization (ECP). $MgCl_2$ solutions with different concentrations were used as the draw solutions while DI water was used as the feed. The volumetric water flux, J_v, and salt flux, J_s, were measured by the weight and conductivity changes in the feed tank using a digital mass balance and a conductivity meter connected to a computer logging system. The operation was performed at room temperature of ~ 23°C.

3. Results and discussion

3.1. Properties of membrane substrates and LBL membranes

The cross-section morphology of the PES hollow fiber substrate is shown in Fig.2 while its main characteristics are listed in Table 1. The substrate used in this study inherits the excellent membrane properties from our previous work [29, 31, 32] with a further modified pore structure. Some key substrate parameters that are favorable for the FO process include high pure water permeability (350 L/h m^2 bar), high porosity (84%), a large fiber lumen size (1080 μm) and straight needle-like pores with very thin sponge-like structure [20, 33]. In addition, the small surface pores with a sharp pore size distribution (mean diameter around 10.9 nm with a standard deviation of 1.04) are beneficial to the subsequent LBL deposition to minimize the polyelectrolytes penetration as well as to increase the deposition homogeneity.

The FTIR spectra shown in Fig. 3 confirms the successful deposition of PSS/PAH layers on the substrate surface where the amine bands were detected around 3420 cm^{-1} for $–NH_2$ group and 2912 cm^{-1} for $–NH_3^+$ group [34]. In addition, one new peak was also observed at 1035 cm^{-1} for the characteristic stretching vibration of the $–SO_3$ group in PSS [26, 34]. This is due to the interpenetration nature of the deposited polyelecolytes, even though the terminated layer was PAH in this case [35].

3.2. Filtration performances of the PES substrate and LBL membranes

The filtration performances of the PES substrate and LBL membranes with a 500 ppm $MgCl_2$ solution are listed in Table 2. A drastic decrease in PWP from 350 to 16.9 L/m^2 h bar was observed upon completing the first two layers deposition, which indicates the effective coverage of the pores on the substrate surface by the polyelectrolytes. The surface pores are believed to be fully covered after three layer deposition. The further increment of the deposition layers only resulted in a slightly drop of the PWP due to increased hydraulic resistance with no significant improvement in the rejection to the $MgCl_2$. Therefore, 3-layer LBL membranes were chosen as the starting candidate for the following FO tests later.

The rejection mechanism of the 6-layer LBL membrane was determined by performing the filtration test against four types of salt solutions (NaCl, Na_2SO_4, $MgSO_4$, $MgCl_2$) as suggested in various studies on NF membranes [36, 37]. The rejection results are shown in Fig.4. It can be seen that the LBL membrane exhibits a high $MgCl_2$ rejection (above 97%) and a very low Na_2SO_4 rejection (less than 5%), indicating its positively charged nature and that Donnan exclusion plays a dominant role in the ion retention at the low salt concentration. In addition to the Donnan effect, the size exclusion also affects the ion rejection in NF. In this experiment, a higher rejection for $MgSO_4$ than NaCl was observed which is probably due to larger hydrated radii of $MgSO_4$ as compared to NaCl (0.43 and 0.38 nm for Mg^{2+} and SO_4^{2-}against 0.36 and 0.33nm for Na^+ and Cl^-) [38]. However, the solute rejection of the LBL membrane is expected to strongly depend on the surrounding ionic strength. In a high ionic strength environment, the enhanced shielding effect can greatly suppress the Donnan exclusion

and thus reduce the salt retention [39]. This is one of the major factors contributing to a distinctive phenomenon observed in the FO performance of NF-like membranes which will be discussed in the next section.

3.3. Performance in FO mode

3.3. 1. AL-facing-DS orientation

The FO performance of the LBL membranes in terms of water flux (J_v) and the reverse salt flux (J_s) as a function of the deposited layer in AL-facing-DS orientation is plotted in Fig. 5A. A 0.5 M $MgCl_2$ solution was used as the draw solution, while the feed was DI water. It was observed that J_v increased from 28 to 40.5 L/m^2 h and J_s decreased from 17.15 to 8.1 g/m^2 h after 6 layers were deposited. With the increment of the deposited layers, the selective layer thickness increased with the formation of a tighter inter-layer structure due to the polyelectrolyte entanglement [40]. As a result, in the FO process, it established a higher osmotic driving force across the membrane due to the reduced salt leakage, and therefore a higher water flux was obtained. Thus, although the increased number of layers would decrease the water permeability (Table 2) this was more than compensated for by the increased driving force. Similar variation trends were observed at various draw solution concentrations ranging from 0.025 to 1 M. One can anticipate better results with a further increment of the deposited layers. However, it is beyond the scope of the current work as it requires a more rigorous deposition protocol to reduce the experimental variations (such as the change of pH and concentration of polyelectrolytes solution) due to the prolonged experiment time [41]. Some deposition methods adopted on flat sheet membranes with the aid of automatic instruments can be found elsewhere [41-43].

The effect of draw solution concentration on a 6-layer LBL membrane is shown in Fig. 5B. Two distinguishable regions of flux increment can be clearly observed at the point around 0.2 M $MgCl_2$ concentration. For charged NF membranes, the salt rejection mechanism is a combination of both Donnan exclusion and size hindrance. As mentioned earlier in Section 3.1.1, at a low draw solution concentration, a high salt rejection was expected due to the strong electrostatic repulsion of the selective layer to the co-ions of Mg^{2+}. Thus, the water flux increased almost linearly with increased osmotic pressure within the first region (from 8.6 L/m^2 h at 0.025 M to 30.2 L/m^2 h at

0.2 M). In the second region, however, the shielding effect on the membrane surface charges caused by the counter-ions of Cl^- became more severe with an elevated draw solution concentration as the selective layer was exposed to the draw solution directly. Therefore, the Donnan exclusion was greatly suppressed, resulting in a significant salt leakage to the feed water. This not only reduced the osmotic pressure difference across the selective layer but also enhanced the concentrative internal concentration polarization (ICP) [44] inside the porous substrate, which further reduced effective osmotic driving force. Consequently, when the concentration of the draw solution increased from 0.5 to 1 M, there was only a marginal increase of water flux (from 40.5 L/m^2 h to 41 L/m^2 h) with a high reverse salt flux (13.47 g/ m^2 h).

3.3. 2. AL-facing-FW orientation

Fig. 6 illustrates the FO performance of the LBL membrane in AL-facing-FW orientation. From Fig.6A we can see that the effect of deposited layers on J_v and J_s in this orientation is not as pronounced as in AL-facing-DS orientation (Fig.5). When the porous substrate was placed against the concentrated draw solution, the dilutive ICP took place in the membrane substrate where the salt concentration at the interior surface of the selective layer was greatly diluted by the convective water flow from the feed side [44]. Thus, the actual salt concentration experienced by the charged membrane surface was much smaller than the bulk solution, leading to a much less shielding effect. Since the degree of the dilutive ICP is mainly determined by the substrate structure, the salt rejection does not vary too much with the increase in the number of deposition layers under the same draw solution concentration.

The dilutive ICP also resulted in a better salt rejection at a high draw solution concentration for the 6-layer LBL membrane in the AL-facing-FW orientation. As shown in Fig. 6B, the salt flux was only 4.1 g/ m^2 h using a 2 M draw solution compared with 13.47 g/m^2 h at 1 M in the AL-facing-DS orientation. As a trade off, the water flux was also much lower (25.63 L/m^2 h) than the previous case due to the smaller effective osmotic gradient across the selective layer.

3.3. 3 Comparison with other NF-like membranes

Table 3 lists the FO performance of the 6-layer LBL hollow fibers along with some NF-like FO membranes from the literature. It can be seen that the LBL hollow fibers exhibited superior performance in both orientations for its high water flux and low salt leakage compared with other NF-like FO membranes under the same test conditions. In particular, reasonably high water fluxes of 14.6 and 25.9 L/m^2 h with corresponding low J_s/J_v ratios of 0.034 and 0.066 g/L can be achieved using 0.05 and 0.1 M draw solution concentrations, respectively, in the AL-facing-DS orientations. These promising results indicate the possibility of substantial reductions of the draw solution replenishment, and the energy consumption for draw solution regeneration and separation using LBL hollow fiber FO membranes. However, the long-term stability of the polyelectrolyte layers has to be ensured for practical applications.

4. Conclusions

The layer-by-layer polyelectrolyte deposition technique has been successfully applied on a PES hollow fiber substrate to make novel LBL hollow fibers for FO application for the first time. A simple deposition procedure involves immersing the substrate into the polyanion PSS and polycation PAH solutions alternately to achieve the desired number of deposition layers.

The newly developed LBL hollow fibers exhibited excellent FO performance. With 6 layers of polyelectrolyte deposited, the membrane showed a high water flux of 40.5 L/m^2 h with a low J_s/J_v ratio of 0.201 g/L when using DI water as the feed and a 0.5 M $MgCl_2$ solution as the draw solutions in the AL-facing-DS orientation. In addition, 14.6 and 25.9 L/m^2 h water fluxes with corresponding low J_s/J_v ratios of 0.034 and 0.066 g/L can be achieved using 0.05 and 0.1 M draw solution concentrations, respectively, in the AL-facing-DS orientations, suggesting great potential of the LBL hollow fibers in the FO process. They should be able to substantially reduce the draw solution replenishment, and the energy consumption for draw solution regeneration and separation.

Acknowledgements

We would like to thank the Singapore Economic Development Board for funding the Singapore Membrane Technology Centre.

References

[1] T.Y. Cath, N.T. Hancock, C.D. Lundin, C. Hoppe-Jones, J.E. Drewes, A multi-barrier osmotic dilution process for simultaneous desalination and purification of impaired water, J. Membr. Sci. 362 (2010) 417-426.

[2] Y.J. Choi, J.S. Choi, H.J. Oh, S. Lee, D.R. Yang, J.H. Kim, Toward a combined system of forward osmosis and reverse osmosis for seawater desalination, Desalination 247 (2009) 239-246.

[3] C.R. Martinetti, A.E. Childress, T.Y. Cath, High recovery of concentrated RO brines using forward osmosis and membrane distillation, J. Membr. Sci. 331 (2009) 31-39.

[4] W.L. Tang, H.Y. Ng, Concentration of brine by forward osmosis: Performance and influence of membrane structure, Desalination 224 (2008) 143-153.

[5] W.C.L. Lay, Y. Liu, A.G. Fane, Impacts of salinity on the performance of high retention membrane bioreactors for water reclamation: a review, Water Res. 44 (2010) 21-40.

[6] E.R. Cornelissen, D. Harmsen, K.F. de Korte, C.J. Ruiken, J.J. Qin, H. Oo, L.P. Wessels, Membrane fouling and process performance of forward osmosis membranes on activated sludge, J. Membr. Sci. 319 (2008) 158-168.

[7] E.M. Garcia-Castello, J.R. McCutcheon, M. Elimelech, Performance evaluation of sucrose concentration using forward osmosis, J. Membr. Sci. 338 (2009) 61-66.

[8] B. Jiao, A. Cassano, E. Drioli, Recent advances on membrane processes for the concentration of fruit juices: a review, J. Food Eng. 63 (2004) 303-324.

[9] T. Cath, A. Childress, M. Elimelech, Forward osmosis: Principles, applications, and recent developments, J. Membr. Sci. 281 (2006) 70-87.

[10] S. Loeb, L. Titelman, E. Korngold, J. Freiman, Effect of porous support fabric on osmosis through a Loeb-Sourirajan type asymmetric membrane, J. Membr. Sci. 129 (1997) 243-249.

[11] J.R. McCutcheon, M. Elimelech, Influence of concentrative and dilutive internal concentration polarization on flux behavior in forward osmosis, J. Membr. Sci. 284 (2006) 237-247.

[12] A. Achilli, T.Y. Cath, A.E. Childress, Selection of inorganic-based draw solutions for forward osmosis applications, J. Membr. Sci. 364 (2010) 233-241.

[13] C.Y.Y. Tang, Q.H. She, W.C.L. Lay, R. Wang, A.G. Fane, Coupled effects of internal concentration polarization and fouling on flux behavior of forward osmosis membranes during humic acid filtration, J. Membr. Sci. 354 (2010) 123-133.

[14] N.Y. Yip, A. Tiraferri, W.A. Phillip, J.D. Schiffman, M. Elimelech, High Performance Thin-Film Composite Forward Osmosis Membrane, Environ. Sci. Technol. 44 (2010) 3812-3818.

[15] J. Wei, C.Q. Qiu, C.Y.Y. Tang, R. Wang, A.G. Fane, Synthesis and characterization of flat-sheet thin film composite forward osmosis membranes, J. Membr. Sci. 372 (2011) 292-302.

[16] W. Fang, R. Wang, S. Chou, L. Setiawan, A.G. Fane, Composite forward osmosis hollow fiber membranes: Integration of RO- and NF-like selective layers to enhance membrane properties of anti-scaling and anti-internal concentration polarization, J. Membr. Sci. 394-395 (2012) 140-150.

[17] S. Chou, R. Wang, L. Shi, Q. She, C. Tang, A.G. Fane, Thin-film composite hollow fiber membranes for pressure retarded osmosis (PRO) process with high power density, J. Membr. Sci. 389 (2012) 25-33.

[18] J. Su, T.S. Chung, B.J. Helmer, J.S. de Wit, Enhanced double-skinned FO membranes with inner dense layer for wastewater treatment and macromolecule recycle using Sucrose as draw solute, J. Membr. Sci. 396 (2012) 92-100.

[19] Q. Yang, K.Y. Wang, T.S. Chung, Dual-Layer hollow fibers with enhanced flux as novel forward osmosis membranes for water production, Environ. Sci. Technol. 43 (2009) 2800-2805.

[20] L. Setiawan, R. Wang, K. Li, A.G. Fane, Fabrication of novel poly(amide–imide) forward osmosis hollow fiber membranes with a positively charged nanofiltration-like selective layer, J. Membr. Sci. 369 (2011) 196-205.

[21] C. Qiu, L. Setiawan, R. Wang, C.Y. Tang, A.G. Fane, High performance flat sheet forward osmosis membrane with an NF-like selective layer on a woven fabric embedded substrate, Desalination 287 (2012) 266-270.

[22] L. Setiawan, R. Wang, K. Li, A.G. Fane, Fabrication and characterization of forward osmosis hollow fiber membranes with antifouling NF-like selective layer, J. Membr. Sci. 394-395 (2012) 80-88.

[23] R. Malaisamy, M.L. Bruening, High-flux nanofiltration membranes prepared by adsorption of multilayer polyelectrolyte membranes on polymeric supports, Langmuir 21 (2005) 10587-10592.

[24] W.Q. Jin, A. Toutianoush, B. Tieke, Use of polyelectrolyte layer-by-layer assemblies as nanofiltration and reverse osmosis membranes, Langmuir 19 (2003) 2550-2553.

[25] K.P. Xiao, J.J. Harris, A. Park, C.M. Martin, V. Pradeep, M.L. Bruening, Formation of ultrathin, defect-free membranes by grafting of poly(acrylic acid) onto layered polyelectrolyte films, Langmuir 17 (2001) 8236-8241.

[26] J. Meier-Haack, W. Lenk, D. Lehmann, K. Lunkwitz, Pervaporation separation of water/alcohol mixtures using composite membranes based on polyelectrolyte multilayer assemblies, J. Membr. Sci. 184 (2001) 233-243.

[27] Q. Saren, C.Q. Qiu, C.Y. Tang, Synthesis and characterization of novel forward osmosis membranes based on layer-by-layer assembly, Environ. Sci. Technol. 45 (2011) 5201-5208.

[28] Y. Xu, X.Y. Peng, C.Y.Y. Tang, Q.S.A. Fu, S.Z. Nie, Effect of draw solution concentration and operating conditions on forward osmosis and pressure retarded osmosis performance in a spiral wound module, J. Membr. Sci. 348 (2010) 298-309.

[29] R. Wang, L. Shi, C.Y. Tang, S. Chou, C. Qiu, A.G. Fane, Characterization of novel forward osmosis hollow fiber membranes, J. Membr. Sci. 355 (2010) 158-167.

[30] J. Ren, Z. Li, F.S. Wong, A new method for the prediction of pore size distribution and MWCO of ultrafiltration membranes, J. Membr. Sci. 279 (2006) 558-569.

[31] S. Chou, L. Shi, R. Wang, C.Y. Tang, C. Qiu, A.G. Fane, Characteristics and potential applications of a novel forward osmosis hollow fiber membrane, Desalination 261 (2010) 365-372.

[32] L. Shi, S.R. Chou, R. Wang, W.X. Fang, C.Y. Tang, A.G. Fane, Effect of substrate structure on the performance of thin-film composite forward osmosis hollow fiber membranes, J. Membr. Sci. 382 (2011) 116-123.

[33] A. Tiraferri, N.Y. Yip, W.A. Phillip, J.D. Schiffman, M. Elimelech, Relating performance of thin-film composite forward osmosis membranes to support layer formation and structure, J. Membr. Sci. 367 (2011) 340-352.

[34] D.L. Pavia, Introduction to spectroscopy, 4th ed., Brooks/Cole, Cengage Learning, Belmont, CA, 2009.

[35] M. Schonhoff, Layered polyelectrolyte complexes: physics of formation and molecular properties, J. Phys. Condens. Matter, 15 (2003) R1781-R1808.

[36] J. Schaep, B. Van der Bruggen, C. Vandecasteele, D. Wilms, Influence of ion size and charge in nanofiltration, Sep. Purif. Technol. 14 (1998) 155-162.

[37] J.M.M. Peeters, J.P. Boom, M.H.V. Mulder, H. Strathmann, Retention measurements of nanofiltration membranes with electrolyte solutions, J. Membr. Sci. 145 (1998) 199-209.

[38] E.R. Nightingale, Phenomenological theory of ion solvation-effective radii of hydrated ions, J. Phys. Chem. 63 (1959) 1381-1387.

[39] M. Teixeira, M. Rosa, M. Nystrom, The role of membrane charge on nanofiltration performance, J. Membr. Sci. 265 (2005) 160-166.

[40] S.T. Dubas, J.B. Schlenoff, Factors controlling the growth of polyelectrolyte multilayers, Macromolecules 32 (1999) 8153-8160.

[41] K.C. Krogman, N.S. Zacharia, S. Schroeder, P.T. Hammond, Automated process for improved uniformity and versatility of layer-by-layer deposition, Langmuir 23 (2007) 3137-3141.

[42] J.B. Schlenoff, S.T. Dubas, Mechanism of polyelectrolyte multilayer growth: Charge overcompensation and distribution, Macromolecules 34 (2001) 592-598.

[43] J. Choi, M.F. Rubner, Influence of the degree of ionization on weak polyelectrolyte multilayer assembly, Macromolecules 38 (2005) 116-124.

[44] G.T. Gray, J.R. McCutcheon, M. Elimelech, Internal concentration polarization in forward osmosis: role of membrane orientation, Desalination 197 (2006) 1-8.

List of Tables

List of Figures

Dimension			Porosity	MWCO	Mean pore size	Standard deviation	Pure water flux	Tensile modulus	Stress at break	Strain at break
OD (μm)	ID (μm)	Thickness (μm)	ε (%)	(kDa)	D^*(nm)	σ	(L/h m^2 bar)	(Mpa)	(Mpa)	%
1480	1080	200	84	39	10.9	1.04	350	70.4	3.64	66

Table 1. Characteristics of PES hollow fiber substrate.

Membrane	Pure water permeability[a] (L/m^2 hbar)	Salt water permeability[a] (L/m^2 hbar)	$MgCl_2$ rejection[a,b] %
Substrate	350	–	–
1-layer	95.4	74.8	40
2-layer	16.9	13.8	92.5
3-layer	9.6	7.2	96
4-layer	9.4	7.1	96.5
5-layer	7.4	5.5	97.8
6-layer	6.1	5.1	97.8

[a] Tested at 1 bar.
[b] $MgCl_2$ solution concentration is 500 ppm.

Table 2. Filtration performances of PES substrate and LBL membranes.

Sample	Water flux (L/m^2 h)	Salt flux/water flux(g/L)	Draw solution	Feed	Orientation	Reference
6-layer LBL membrane	14.6	0.034	0.05 M $MgCl_2$	Dl water	AL-facing-DS	Present work
	25.9	0.066	0.1 M $MgCl_2$	Dl water	AL-facing-DS	Present work
	40.5	0.201	0.5 M $MgCl_2$	Dl water	AL-facing-DS	Present work
CA double-skinned hollow fiber	15.7	0.06	0.5 M $MgCl_2$	Dl water	AL-facing-DS	[18]
PAI-PEI crosslinked hollow fiber	13.13	0.7	0.5 M $MgCl_2$	Dl water	AL-facing-DS	[20]
LBL flat sheet	25.1	0.568	1.0 M $MgCl_2$	Dl water	AL-facing-DS	[27]
Dual-layer PBI hollow fiber	15.6	0.038	2.0 M $MgCl_2$	Dl water	AL-facing-DS	[19]
6-layer LBL membrane	18.44	0.113	0.5 M $MgCl_2$	Dl water	AL-facing-FW	Present work
	20.66	0.138	1.0 M $MgCl_2$	Dl water	AL-facing-FW	Present work
PAI-PEI crosslinked hollow fiber	8.36	0.3	0.5 M MgCl2	Dl water	AL-facing-FW	[20]
LBL flat sheet	22	0.302	1.0 M MgCl2	Dl water	AL-facing-FW	[27]
Dual-layer PBI hollow fiber	7.5	0.053	2.0 M MgCl2	Dl water	AL-facing-FW	[19]

Table 3. Comparison of various NF-like membranes in FO process.

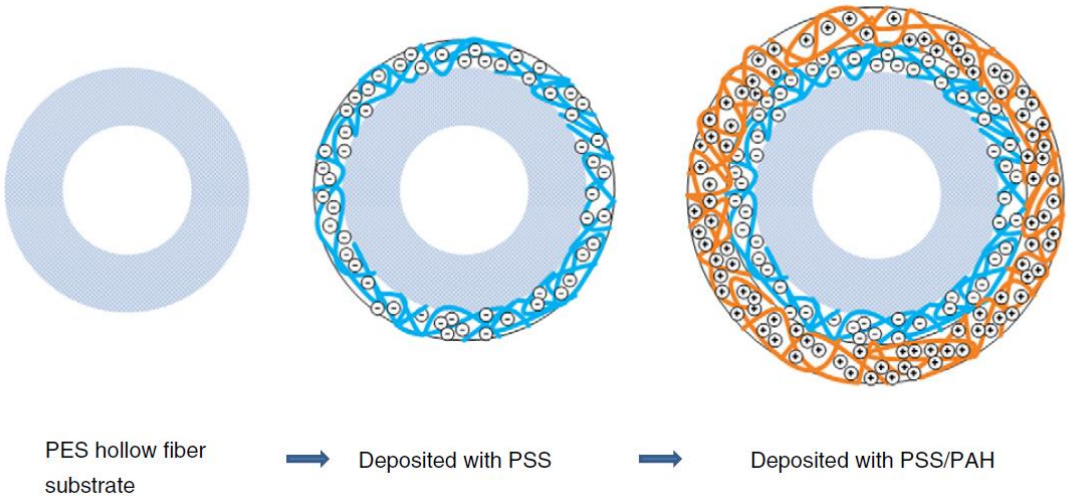

Fig.1. Schematic drawing of layer-by-layer deposition on hollow fiber membrane.

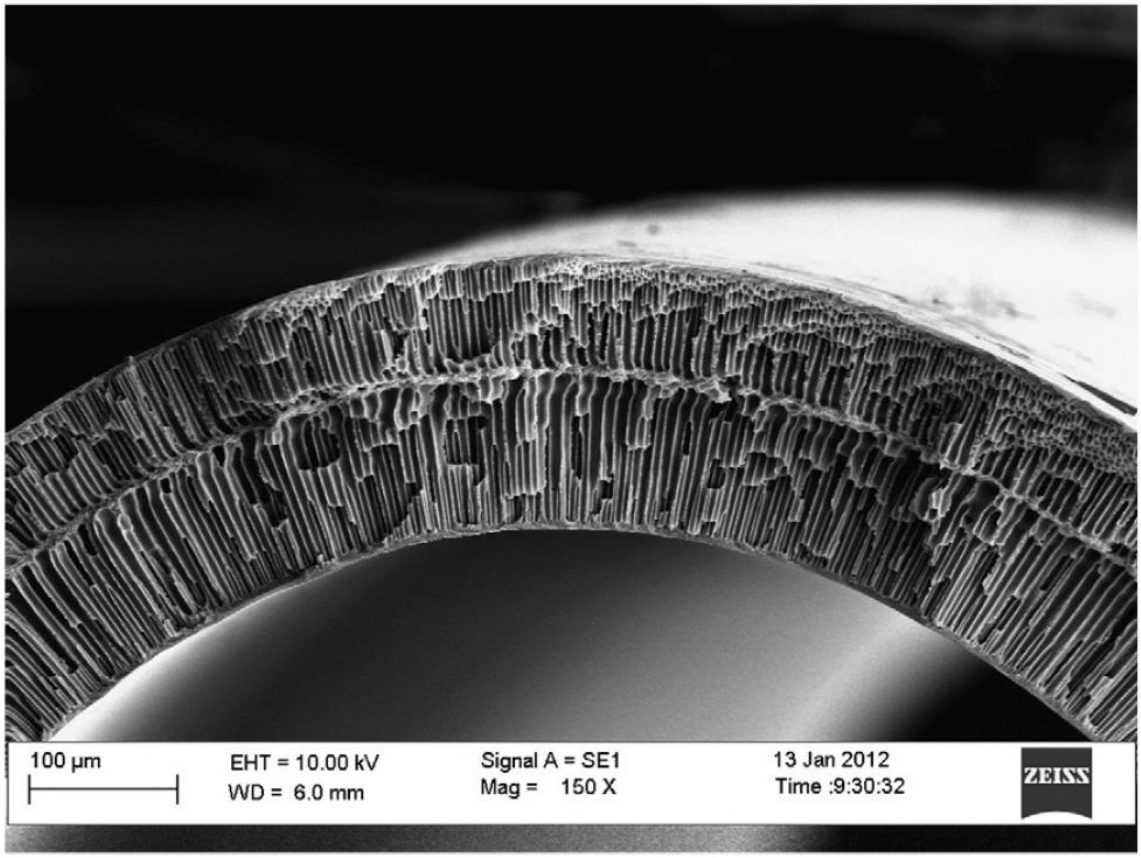

Fig.2. Cross-section morphology of PES hollow fiber substrate at 150x.

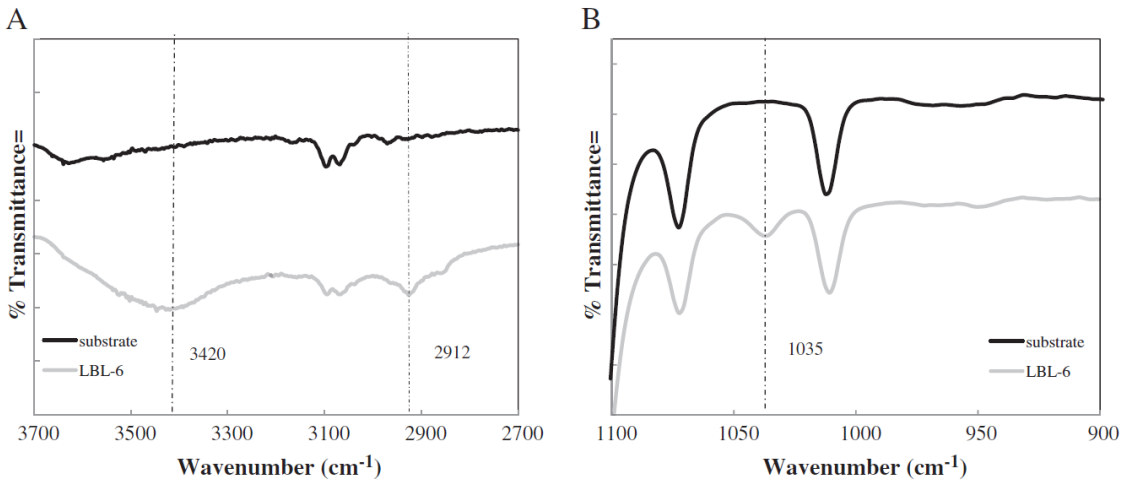

Fig.3. ATR-FTIR spectra of membrane substrate and 6-layer LBL membrane. (A) Indicative peaks of PAH at 3420 cm^{-1} and 2912 cm^{-1}. (B) Indicative peak of PSS at 1035 cm^{-1}.

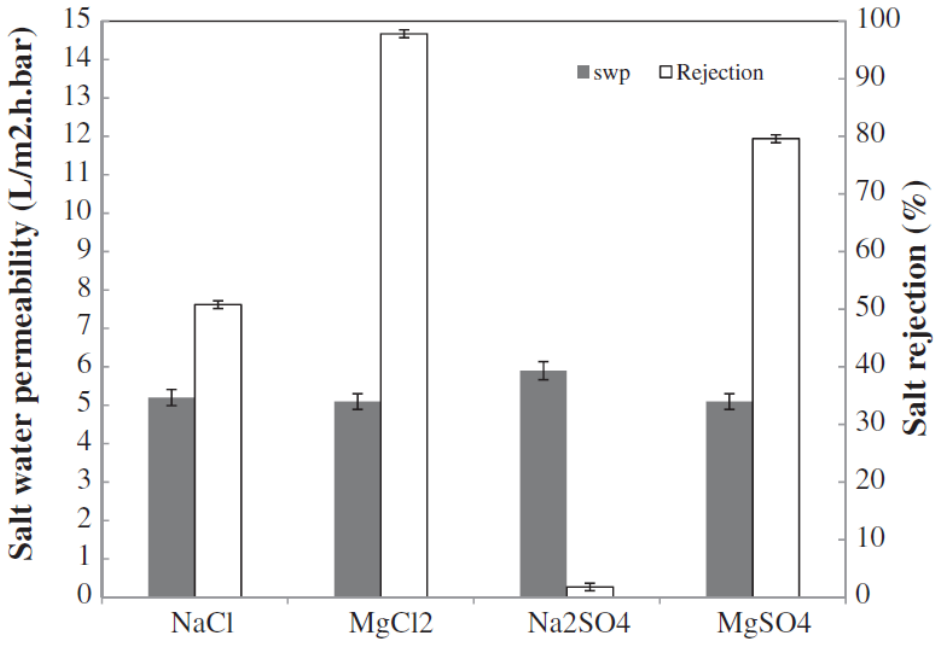

Fig.4. Filtration performances of 6-layer LBL membrane with different salt solutions (tested at 1 bar using 500 ppm salt solution).

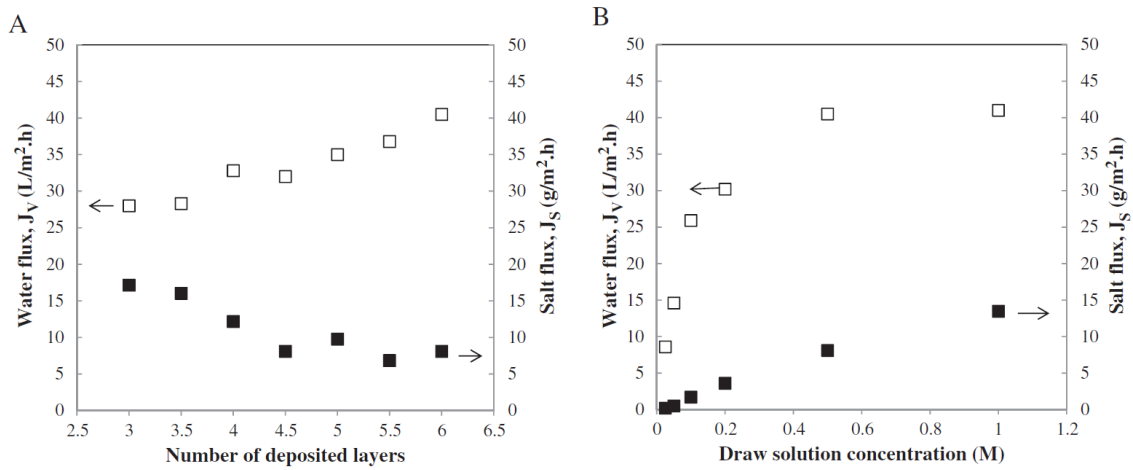

Fig.5. FO performance of LBL membrane in AL-facing-DS orientation (□:J_v,■J_s). (A) Effect of deposited layers using 0.5 M $MgCl_2$ as draw solution. (B) Effect of draw solution concentration on 6-layer LBL membrane.

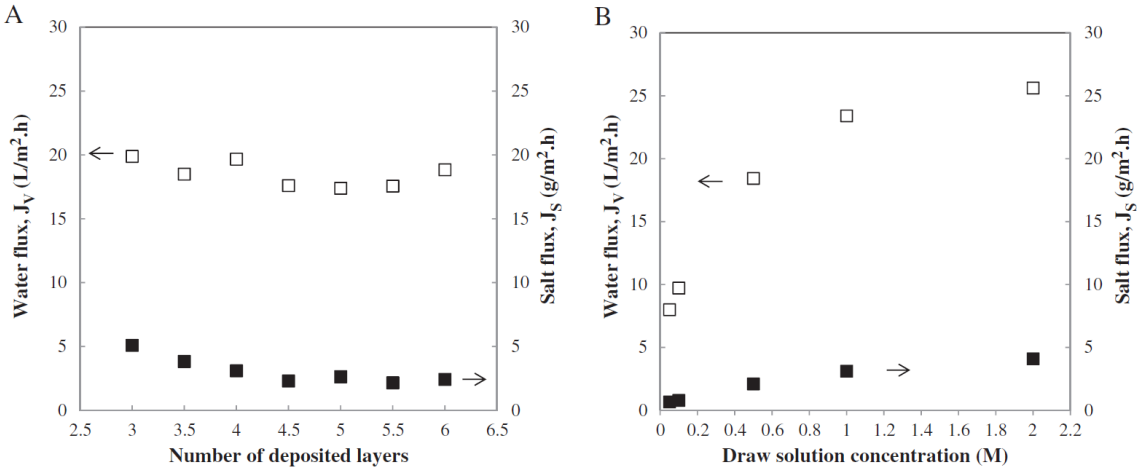

Fig.6. FO performance of LBL membrane in AL-facing-FW orientation (□:J_v,■J_s). (A) Effect of deposited layers using 0.5 M $MgCl_2$ as draw solution. (B) Effect of draw solution concentration on 6-layer LBL membrane.